Journal of Applied Polymer Science

Nylon 6/Multiwalled Carbon Nanotube Composites: Effect of the Melt-Compounding Conditions and Nanotube Content on the Morphology, Mechanical Properties, and Rheology

Florian Puch, Christian Hopmann
Institute of Plastics Processing at RWTH Aachen University, Seffenter Weg 201, 52074 Aachen, Germany
Correspondence to: F. Puch (E-mail: florian.puch@rwth-aachen.de)

ABSTRACT: The effect of the melt-compounding conditions with the use of a corotating intermeshing twin-screw extruder and of the nanotube content on the morphology and the mechanical and rheological properties of nylon 6/multiwalled carbon nanotube (MWCNT) composites was investigated. The melt-compounding conditions affected the morphology, but the variations in the morphology did not necessarily result in substantial variations in the mechanical and rheological properties. The mass throughput had the strongest influence on the mechanical properties, whereas the MWCNT feeding substantially affected the rheology. The increase in the MWCNT volume content from 0.0 to 3.5 vol % led to an increase in the Young's modulus, whereas the tensile strength, elongation at break, and notched impact strength exhibited maximum values around 0.5 to 1.0 vol %. With increasing MWCNT volume contents, higher complex viscosities and storage and loss moduli and a lower loss factor compared to neat nylon 6 were observed.
 J. Appl. Polym. Sci. **2014**, *131*, 40893.

KEYWORDS: extrusion; mechanical properties

Received 14 February 2014; accepted 17 April 2014
DOI: 10.1002/app.40893

INTRODUCTION

Nylon 6 is among the most important technical thermoplastic polymers, as it comes with decent material properties such as a high strength and stiffness. Major applications of nylon 6 are found in the fiber sector and in the automotive, aviation, and electrical/electronics industries. To enhance the material properties of nylon 6, it is often filled with fillers, such as glass or carbon fibers.[1,2] Because of the high filler contents necessary to further improve the composite properties, the potential of these fillers on micrometer scale is limited.[3] However, for more than 20 years, another class of fillers, fillers on the nanometer scale [e.g., carbon nanotubes (CNTs) and layered silicates], have been investigated.[4–7] Most of the so-called nanofillers feature a high surface-to-volume-ratio. Together with an adequate surface chemistry of the filler, both a high specific surface area and a good compatibility allow a large area of interaction for the polymer and the filler to build physical bonds; this results in a high potential to improve the polymer–nanocomposite properties, even at low filler contents.[8]

Polymer–nanocomposites can be prepared by solution processing, *in situ* polymerization, or melt compounding. Despite the fact that these methodologies are different, they all target the deagglomeration of nanofiller agglomerates, good dispersion, and interfacial bonding to obtain optimum polymer–nanocomposite properties.[9,10] The most important route for the preparation of polymer–nanocomposites in industry is melt compounding with a corotating intermeshing twin-screw extruder.[11] Thus, in this study, we focused on the influence of the melt-compounding conditions on the morphology, mechanical properties, and rheology of nylon 6 nanocomposites to allow a transfer of the scientific findings to industrial practice.

Featuring a high scientific and industrial interest, CNTs are among the most important nanofillers. Multiwalled carbon nanotubes (MWCNTs), in particular, are already manufactured on an industrial scale. Hence, the properties of CNTs and polymer–CNT–composites and the scientific progress have been summarized and discussed in several review articles.[10,12–29]

Concerning specifically the properties of the nylon 6/MWCNT composites prepared by melt mixing, Zhang et al.[30] observed an increase in the Young's modulus and tensile strength by 120 and 115%, respectively. The nylon 6/MWCNT composites filled with 1 wt % MWCNTs were prepared with a small laboratory kneader. Liu et al.[31] even reported an increase in the Young's modulus of 214% and an increase in the tensile strength of 162% with the addition of 2 wt % MWCNTs to nylon 6 in a laboratory twin-screw extruder, which melt-mixed the materials

for 10 min at 250°C with a screw rotational speed of 100 1/min. A study of Meng et al.[32] showed less pronounced improvements in the mechanical properties. However, in all of the studies mentioned previously, laboratory-scale mixing equipment was used; this equipment cannot be directly scaled up to an industrial scale because of a lack in geometric and heat-transfer similarity. Meincke et al.[33] observed an increase in Young's modulus with increasing MWCNT content (2–12 wt %), whereas the elongation at break decreased. Young's modulus improved by about 40% for a nanocomposite containing 6 wt % MWCNTs. Furthermore, the complex viscosity, storage modulus (G'), and loss modulus (G'') increased with the addition of MWCNTs to nylon 6. This effect was attributed to the restricted chain mobility and orientation of the nylon 6 chains.[34,35] The results reported in literature were in good agreement with the properties obtained in this study. In principle, the publications named previously already indicated that the melt-mixing conditions play an important role in the resulting properties of nylon 6/MWCNT composites because the MWCNTs have to be individualized to fully benefit from the superior properties of the MWCNTs. Otherwise, the MWCNT agglomerates act as defects in the polymeric matrix.[9]

In literature, a large number of researchers have reported investigations of small-scale melt-mixing processes; these have revealed for different polymers, including nylon 6, that high shear forces and relatively long mixing times promote the individualization of MWCNTs.[36–47] On the basis of laboratory-scale experiments, Kasaliwal et al.[48] proposed a kinetic model for the dispersion of MWCNTs in polymers by melt mixing. This model describes the dispersion of MWCNT agglomerates on the basis of the mechanisms rupture and erosion. In this model, MWCNT agglomerates are divided in two classes: large agglomerates with a diameter of larger than 10 μm and small agglomerates between 1 and 10 μm. Large agglomerates are believed to undergo rupture and erosion, whereas small agglomerates are mostly dispersed by erosion during melt mixing.[48] Villmow and coworkers[11,49] reported two studies on the influence of the melt-compounding process parameters with a corotating intermeshing twin-screw extruder. Their studies on polycaprolactone–MWCNT and polylactide–MWCNT composites showed that high screw rotational speeds, screw configurations with distributive mixing elements, and longer residence times led to an enhanced dispersion of MWCNTs, whereas high throughputs worsened the dispersion of MWCNTs. The temperature profile was observed to have a minor effect on the MWCNT dispersion. However, still higher processing temperatures resulted in a slightly better dispersion of the MWCNTs. However, both publications focused on the dispersion of MWCNTs and the electrical conductivity of the composites, whereas the mechanical and rheological properties were not investigated. Sathyanarayana et al.[50] observed similar effects regarding the screw rotational speed in their study on polystyrene–MWCNT composites. Furthermore, their investigations revealed only a small effect of the process parameters on the rheological properties of the prepared nanocomposites. Finally, a study from Guehenec et al.[51] concluded that the MWCNT dispersion may not have further improved above a screw rotational speed of 200 min^{-1}, which was also reflected in an optimum of the electrical conductivity.

Thus, the influence of the process parameters during melt mixing with a corotating intermeshing twin-screw extruder on the morphology and the mechanical and rheological properties of nylon 6/MWCNT composites have not been described in the literature so far. Hence, the aim of this study was to examine the morphology and the mechanical and rheological properties of these nanocomposites in different melt-compounding conditions. Additionally, in dependency of the MWCNT content on the aforementioned properties is described.

EXPERIMENTAL

Materials

Different nanocomposites consisting of the matrix polymer nylon 6 and MWCNT nanofillers were prepared in this study. The matrix polymer nylon 6 (type Ultramid B27E01) was provided by BASF SE (Ludwigshafen, Germany). Being a typical compounding grade, it had a relative viscosity of 2.7 and a density of 1.13 g/cm^3.[52] The MWCNTs (type NC7000) were provided by Nanocyl S. A. (Sambreville, Belgium). They had an average diameter of 9.5 nm and an average length of 1.5 μm. The surface area was 250 to 300 m^2/g.[53] Figure 1 shows the scanning electron microscopy (SEM) images of the MWCNTs at different magnifications.

The SEM images indicated the presence of two MWCNT agglomerate size classes, as described by Kasaliwal et al.[48] because the large agglomerates consisted of small agglomerates (aggregates) of MWCNTs [Figure 1(a–c)], whereas the small agglomerates were built of individual MWCNTs [Figure 1(d–f)]. The density of the MWCNTs was 1.75 g/cm^3.[54]

Methods

Nylon 6/MWCNT composites containing 1 vol % MWCNTs were prepared with a corotating, intermeshing twin-screw extruder (type ZSK26Mc, Coperion GmbH, Stuttgart, Germany). The screw diameter of the extruder was 26 mm, and the length-to-diameter ratio was 45. During the melt-compounding trials, the nylon 6 was added to the main hopper, whereas the MWCNTs were fed into the fourth barrel element with a side feeder. To investigate the influence of the MWCNT feeding position, the MWCNTs were also fed into the main hopper for comparison. All of the materials were dosed by suitable gravimetric dosing systems. The material was vented before it exited the extruder die as strands. The strands were quenched in a water bath and pelletized by a strand pelletizer.

During melt compounding, the process parameter, mass throughput (10, 20, and 30 kg/h), screw rotational speed (500, 700, and 900 min^{-1}), and screw configuration, were varied in three steps, whereas two barrel temperature profiles and two MWCNT feeding positions were applied. The screw configurations and two barrel temperature profiles are shown in Figure 2.

The three screw configurations featured the same feeding and melting zone for nylon 6, which was built of conveying elements and three-flighted kneading elements, respectively. The dispersive mixing zone, which followed the MWCNT side-feeding zone, was varied to achieve different shear energy inputs in this zone. Screw configuration A had no kneading elements in this zone, and this led to a low-shear-energy input. To achieve a

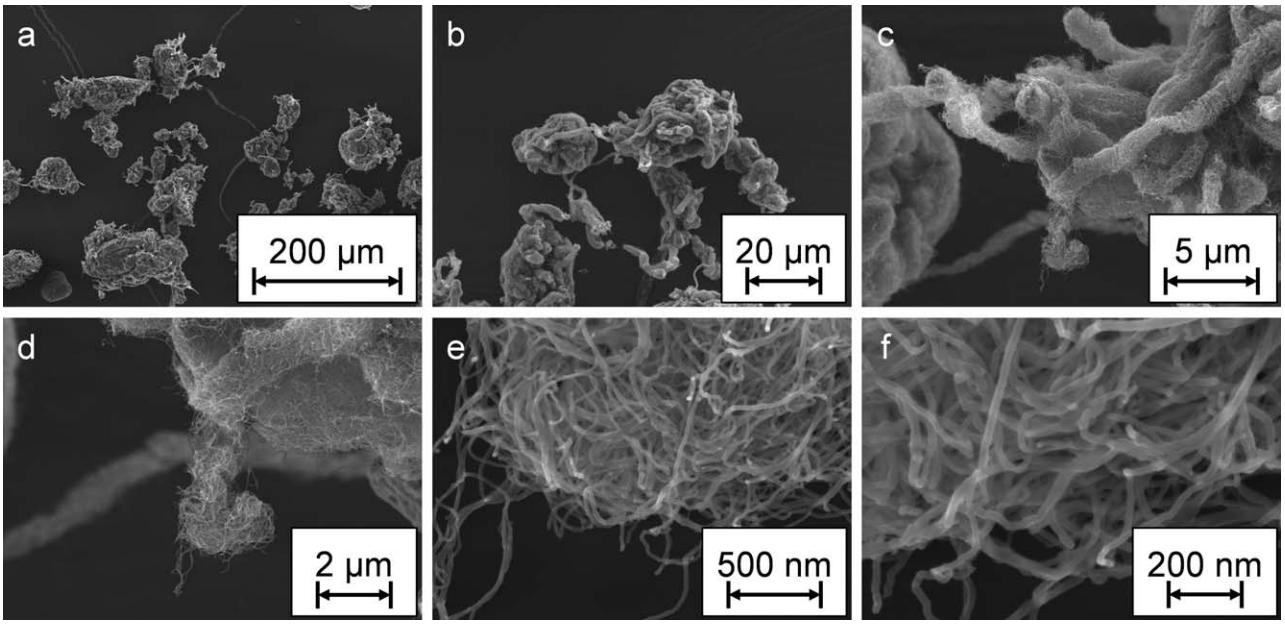

Figure 1. SEM images of the used MWCNTs at different magnifications.

medium-shear-energy input and a partially filled zone, screw configuration B featured five conveying kneading elements in the dispersive mixing zone. Screw configuration C was built up of two sections with kneading elements in the dispersive mixing zone. Both sections ended with a neutral kneading block to achieve a fully filled section, and this resulted in a high-shear-energy input. After each dispersive mixing zone, a distributive mixing zone consisting of 2 × 2 tooth-mixing elements followed. Furthermore, each screw configuration was completed by a venting zone built up of conveying elements. Both the distributive mixing zone and the venting zone were identical for the three screw configurations. During the trials, the utilization (U) of the twin-screw extruder was recorded, and the specific mechanical energy (SME) input was calculated from it according to eq. (1):[55]

$$\mathrm{SME} = \frac{2 \cdot \pi \cdot n \cdot M_D}{\dot{m}} \tag{1}$$

where n is the screw rotational speed and $\dot{m}$ is the mass throughput. The applied torque by the twin-screw extruder (M_D) was determined according to eq. (2):

$$M_D = (U - U_0) \cdot M_{\max} \tag{2}$$

where U_0 is the utilization of the twin-screw extruder during idle running and $M_{\max}$ is the maximum torque that can be applied by the twin-screw extruder and which accounts for 212

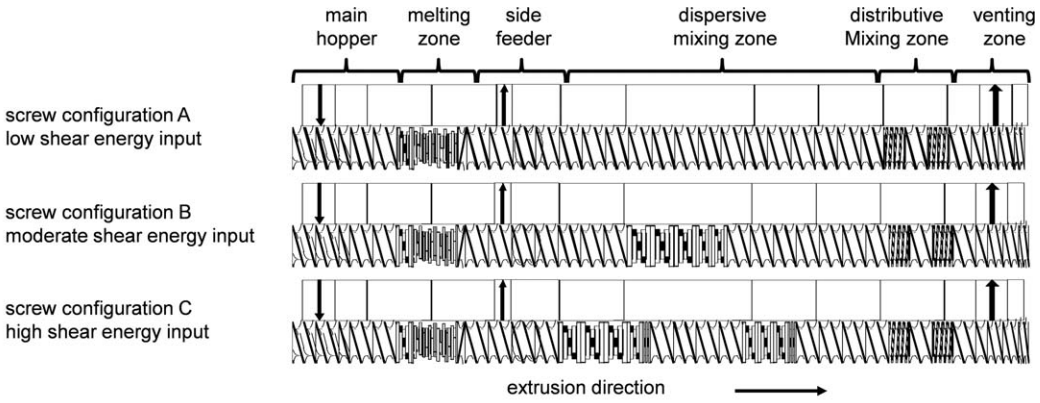

	1	2	3	4	5	6	7	8	9	10	11
low barrel temperature profile [°C]	80	160	200	220	240	240	240	240	240	240	240
high barrel temperature profile [°C]	80	160	200	220	290	290	290	290	290	290	290

Figure 2. Screw configurations and barrel temperature profiles used for melt compounding.

Table I. Influence of the Process Parameters on the SME Input and Mean Residence Time

Mass throughput (kg/h)	Screw rotational speed (min^{-1})	Screw configuration (—)	Barrel temperature profile (—)	MWCNT feeding position (—)[a]	SME (W h/kg)	Mean residence time (s)
10	700	B	Low	SF	435.13	52.0
20	700	B	Low	SF	338.00	26.5
30	700	B	Low	SF	316.73	20.5
20	500	B	Low	SF	313.03	32.0
20	900	B	Low	SF	388.51	23.0
20	700	A	Low	SF	338.00	26.0
20	700	C	Low	SF	361.31	31.0
20	700	B	High	SF	338.00	26.5
20	700	B	Low	MH	396.28	34.0

[a] SF, side feeder; MH, main hopper.

N m. Furthermore, the mean residence time was determined with colored tracer particles, which were added to the pure nylon 6 under the respective melt-compounding conditions before the MWCNTs were dosed. The time when the color appeared and the time when the color disappeared were stopped to calculate the mean residence time from five residence time measurements, which were conducted for each set of process parameters. After we investigated the melt-compounding processing conditions, nylon 6/MWCNT composites containing different MWCNT volume contents were prepared at a mass throughput of 10 kg/h and a screw rotational speed of 500 1/min with screw configuration B and a low-barrel-temperature profile. The nylon 6/MWCNT composites contained MWCNT contents between 0.0 and 3.5 vol %. The MWCNT content was varied in steps of 0.5 vol %.

After melt compounding, the nylon 6/MWCNT composites were processed to test specimens by injection molding with an injection-molding machine (type Allrounder 370 A 600-170/170, Arburg GmbH & Co. KG, Loßburg, Germany). During injection molding, the process parameters were kept constant to maintain the comparability of the composites prepared under different melt-compounding conditions. The mechanical properties, Young's modulus, tensile strength, and elongation at break, of 10 samples were examined according to EN ISO 527 with a tensile testing machine (type Z100, Zwick GmbH & Co. KG, Ulm, Germany). The notched impact strength of 10 samples was determined according to EN ISO 179 with a pendulum (Zwick GmbH & Co. KG). The rheological properties were evaluated with a plate–plate rheometer (type Haake Mars 2, Thermo Fisher Scientific, Inc., Waltham, MA). The frequency sweep was performed at a temperature of 240°C with an amplitude of 2% (0.002 rad) from high frequency (100 Hz) to low frequency (0.1 Hz). Before testing, all of the test specimens were dried (for 7 days at 80°C) to ensure uniform testing conditions. Additionally, the morphology of the samples was investigated on a microscopic scale with optical microscopy to determine the size and number of the remaining MWCNT agglomerates. To quantify the size and number of the remaining MWCNT agglomerates in the nylon 6/MWCNT composites, polished sections were prepared, and overexposed images were taken at a 1000× magnification with a digital microscope (type VHX 600, Keyence Corp., Osaka, Japan). The images were analyzed with the image processing and analysis software ImageJ, and the size and number of the remaining MWCNT agglomerates (black spots in the microscopy image) were measured. From these values, the accumulated agglomerate frequency was calculated by the addition of the number of occurring agglomerates in one size class starting from the biggest agglomerates and proceeding to agglomerates measuring 1 μm^2. The MWCNTs were considered to be dispersed when the size of the agglomerate was smaller than 1 μm^2. Additionally, the nylon 6/MWCNT composites containing different MWCNT volume contents were analyzed by transmission electron microscopy (TEM).

RESULTS AND DISCUSSION

Effect of Melt Compounding

SME Input and Residence Time. As eq. (1) shows, the SME was influenced by the processing conditions during melt compounding. Thus, Table I summarizes the SME versus the process parameter mass throughput, screw rotational speed, screw configuration, barrel temperature profile, and MWCNT feeding position.

As shown in Table I, the SME and mean residence time strongly decreased with increasing throughput; this led to less energy being available for mixing and a shorter mixing time. However, we had to consider that the filling degree of the screws increased with increasing mass throughput; this led to an increase in the local stress transferred onto the MWCNT agglomerates. Increasing the screw rotational speed resulted in an increase in the SME and a decrease in the mean residence time. The application of conveying kneading elements on screw configuration B did not affect the SME and the mean residence time substantially compared to screw configuration A, but the use of neutral kneading elements, which increased the filling degree of the screws, led to an increase in both the SME and the mean residence time. However, the effects of the screw rotational speed and the screw configuration were less pronounced than the effect of the mass throughput. Increasing the barrel

temperature profile did not affect the SME and mean residence time, but it increased the material temperature and resulted in a lower viscosity. Hence, better wetting and infiltration of the agglomerates could be achieved with the high-barrel-temperature profile. Feeding the MWCNT over the main hopper instead of the side feeder led to increases in the SME and mean residence time. Moreover, we considered that the MWCNT interacted with the solid nylon 6 granules until they were molten; this may have resulted in a degradation or compression of the MWCNTs to new agglomerates.[56]

Morphology. Figure 3 shows the accumulated agglomerate frequency in the nylon 6/MWCNT composites versus the mass throughput [Figure 3(a)], the screw rotational speed [Figure 3(b)], screw configuration [Figure 3(c)], barrel temperature profile [Figure 3(d)], and feeding position of the MWCNT [Figure 3(e)]. During the trials, the processing parameters other than those depicted in the figures were kept constant.

In general, in all of nylon 6/MWCNT composites, MWCNT agglomerates were present. Approximately 90% of the MWCNT agglomerates were smaller than 8 μm^2, regardless of the selected melt-compounding conditions. Slightly smaller MWCNT agglomerates were observed when a mass throughput of 30 kg/h was chosen, even though the residence time of the material in the twin-screw extruder was shorter. However, because the filling degree was higher at higher mass throughputs, the shear stresses transferred on the MWCNTs in the dispersive mixing zone may have been higher; this resulted in slightly smaller MWCNT agglomerates left in the nanocomposite. However, Villmow et al.[49] reported worse MWCNT dispersion when they increased the mass throughput during melt compounding,[49] and Sathyanarayana et al.[50] observed no influence of the mass throughput on the MWCNT dispersion. However, in both studies, the melt-compounding processes were operated at lower mass throughputs of 5–15 kg/h[49] and 7.5 to 10 kg/h,[50] respectively; this led to a more pronounced influence of the residence time in the study of Villmow et al.,[49] whereas the difference in the mass throughput may have been too small in the investigation of Sathyanarayana et al.[50] for them to see a substantial difference in the MWCNT dispersion.[50]

Only small differences in the agglomerate size distributions were observed when the screw rotational speed was varied. The smallest number of large agglomerates was noticed at a high screw rotational speed of 900 min^{-1}; this resulted in high shear stresses acting on the MWCNT agglomerates and led to a slightly better dispersion. A similar effect was reported by Villmow et al.[11,49] and Sathyanarayana et al.,[50] when they increased the screw rotational speed from 100 to 500 min^{-1} and from 500 to 1100 1/min,[50] respectively. Also, in all studies, the improvement of the MWCNT dispersion was attributed to the higher shear stresses acting on the MWCNT agglomerates.[11,49,50]

Between screw configurations B and C, only small differences were observed: As expected, the application of neutral kneading elements resulted in slightly smaller MWCNT agglomerates. For screw configuration A, a comparably high number of MWCNT agglomerates larger than 12 μm^2 was observed. However, with decreasing MWCNT agglomerate size, the number of small agglomerates increased; this led to a higher number of agglomerates between 2 and 6 μm^2 than for screw configurations B and C. This effect may have been due to the shear thinning behavior of the nylon 6 because, for screw configurations B and C, higher shear stresses were introduced between the tips of the kneading elements. This led to a local decrease in the melt viscosity and may have resulted in a less effective MWCNT agglomerate dispersion on the one hand. On the other hand, dispersive mixing elements may have led to an MWCNT deterioration; this could result in an increased tendency to form new agglomerates. Similar observations were made by Guehenec et al.[51] when they compared a screw configuration with conveying screw elements to a screw configuration with counterconveying screw elements and by Villmow et al. when they compared a screw configuration with dispersive mixing elements to a screw configuration with distributive mixing elements.[49]

Increasing the barrel temperature led to a slight improvement in the MWCNT dispersion. Thus, a higher number of small agglomerates was detected than in the low barrel temperature profile. This effect was probably due to a decreased melt viscosity; this led to the better wetting and infiltration of the MWCNT agglomerates and, hence, to a decrease in the agglomerate size. However, the decrease in the melt viscosity was believed to be less pronounced than the local decrease in the melt viscosity between the tips of the kneading elements. Villmow et al.[49] also observed a slight improvement in the MWCNT dispersion when the barrel temperature was increased; this was attributed to promoted agglomerate infiltration at higher processing temperatures,[11] whereas Sathyanarayana et al.[50] observed no effect of the processing temperature.

The investigation of the influence of the MWCNT feeding position on the accumulated MWCNT agglomerate frequency showed that a higher number of smaller agglomerates was detected when the MWCNT were fed over the main hopper. Instead of 90% of the remaining MWCNT agglomerates being less than 8 μm^2 in size as observed with the side feeder, 90% of the remaining MWCNT agglomerates exhibited a size of 5 μm^2 or less when the MWCNT were added into the main hopper. This effect occurred because the MWCNTs had to pass the melting zone in addition to the dispersive mixing zone, and this led to a longer residence time and increased the shear stresses acting on the MWCNT agglomerates because the melting zone was built up of three-flighted kneading elements and strong solid–solid and solid–highly viscous liquid interactions took place in the melting zone. However, the MWCNT addition into the main hopper may also have led to a deterioration of the MWCNTs, which was observed by Andrews et al.[37] for high-shear-energy inputs in small-scale mixing. Furthermore Müller et al.[56] reported a worse MWCNT dispersion when they added MWCNTs into the main hopper instead of into a side feeder. This effect was attributed to the compression of the MWCNTs in the feeding and melting zones; this compression led to an increasing number of MWCNT agglomerates even before MWCNT dispersion took place.

The investigations on the influence of the melt-compounding conditions on the morphology on microscopic

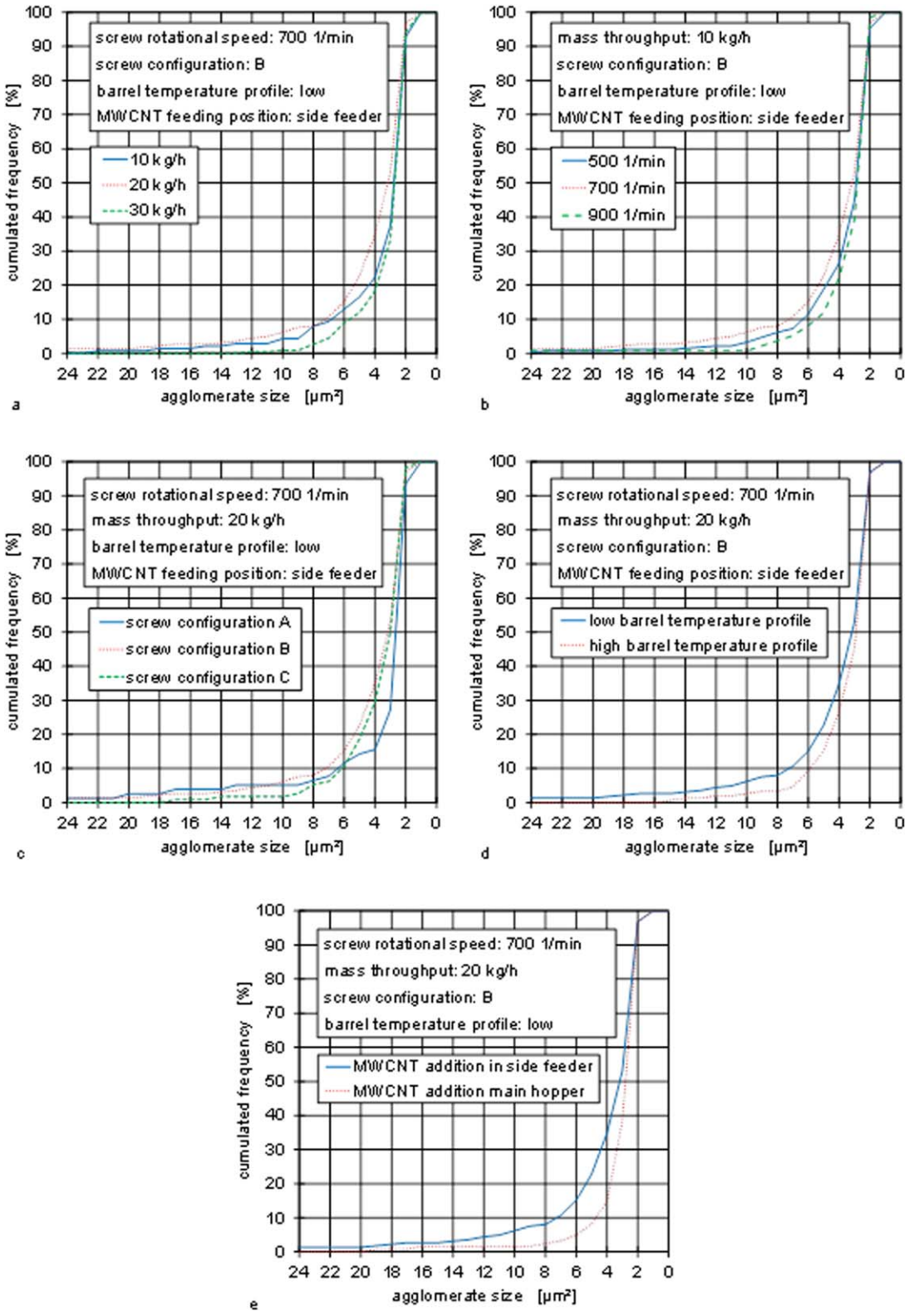

Figure 3. Cumulated MWCNT agglomerate frequencies in the nylon 6/MWCNT composites versus the melt-compounding conditions. [Color figure can be viewed in the online issue, which is available at wileyonlinelibrary.com.]

scale revealed that the compounding process parameters affected the size and number of the remaining MWCNT agglomerates slightly. However, to gather more information, the dispersion of the MWCNTs on a submicroscopic scale should be considered, which until now, has been a big challenge.

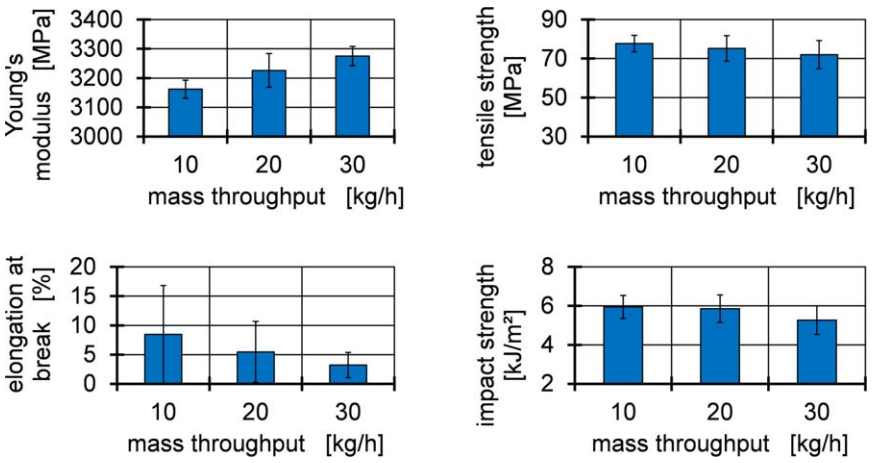

Figure 4. Mechanical properties of the nylon 6/MWCNT composites versus the mass throughput. [Color figure can be viewed in the online issue, which is available at wileyonlinelibrary.com.]

Mechanical Properties. The influence of the mass throughput on the mechanical properties, the Young's modulus, tensile strength, elongation at break, and notched impact strength, is shown in Figure 4. The process parameters, the screw rotational speed (700 1/min), screw configuration B, barrel temperature profile (low), and MWCNT feeding position (side feeder), remained constant.

Increasing the mass throughput led to an increase in Young's modulus, whereas the tensile strength showed a slight tendency to decrease. Furthermore, both the elongation at break and notched impact strength decreased with increasing throughput. However, the differences in the tensile strength and the elongation at break were well within the standard deviation. Thus, they could not be considered substantial. However, the standard deviation of the elongation at break decreased with increasing throughput; this may have been due to a better and more stable dispersion, according to Alig et al.[9] The higher number of smaller agglomerates (see Figure 3) explained the increase in Young's modulus on the one hand.[8] On the other hand, the higher number of agglomerates on a micrometer scale may have caused a higher number of potential defects during impact loading; this resulted in a decrease in the notched impact strength.

Figure 5 presents the influence of the screw rotational speed on the mechanical properties. All of the other process parameters were kept the same (mass throughput = 20 kg/h, screw configuration B, low barrel temperature profile, MWCNT feeding with the side feeder).

The screw rotational speed did not exhibit a substantial influence on the mechanical properties, the Young's modulus, tensile strength, and notched impact strength, remained constant, whereas the elongation at break showed a tendency to increase with increasing screw rotational speed. However, an increase in the standard deviation was observed as well; this was considered by Alig et al.[9] to indicate worse and less stable MWCNT dispersion.

In Figure 6, the mechanical properties are depicted versus the screw configuration. During the experiments, the mass throughput and screw rotational speed were set to 20 kg/h and 700

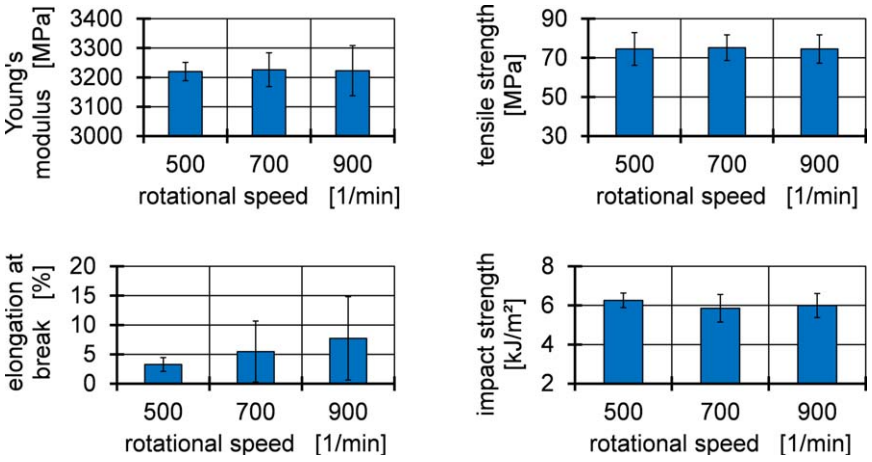

Figure 5. Mechanical properties of the nylon 6/MWCNT composites versus the screw rotational speed. [Color figure can be viewed in the online issue, which is available at wileyonlinelibrary.com.]

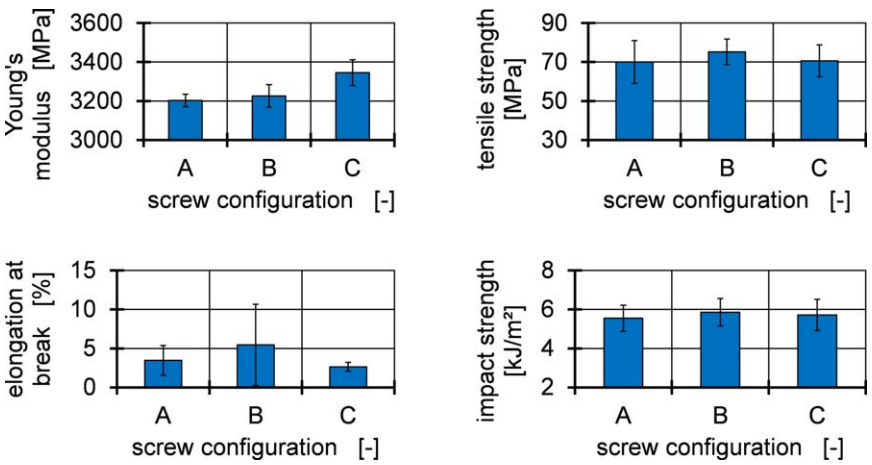

Figure 6. Mechanical properties of the nylon 6/MWCNT composites versus the screw configuration. [Color figure can be viewed in the online issue, which is available at wileyonlinelibrary.com.]

min^{-1}, respectively. Additionally, the low barrel temperature profile was applied. The MWCNTs were fed into a side feeder.

For the mechanical properties, the tensile strength, elongation at break, and notched impact strength, no substantial influence of the screw configuration was observed, even though an increase in the elongation at break was detected for screw configuration B. However, this difference was well within the standard deviation. Only the Young's modulus showed a tendency to increase with increasing shear energy input by the screw configuration; this may have been due to the smaller number of large agglomerates observed with increasing shear energy input by the screw configuration (see Figure 3).

Figure 7 shows the influence of the barrel temperature profile on the mechanical properties. The other process parameters, the mass throughput (20 kg/h), screw rotational speed (700 min^{-1}), screw configuration B, and MWCNT feeding position (side feeder), remained constant.

The tensile strength and elongation at break remained unaffected by the barrel temperature profile, whereas the Young's modulus tended to increase, and the notched impact strength tended to decrease with increasing processing temperature. This effect may be have been due again to the higher number of smaller agglomerates (see Figure 3), which may have caused an increase in the Young's modulus on the one hand[8] and a higher number of potential defects during impact loading on the other hand; this resulted in a decrease in the notched impact strength.

The influence of the MWCNT feeding position on the mechanical properties is presented in Figure 8. All of the other process parameters were kept constant (mass throughput = 20 kg/h, screw rotational speed = 700 min^{-1}, screw configuration B, low barrel temperature profile).

The MWCNT feeding position had no influence on the Young's modulus and the tensile strength, whereas the elongation at break and the notched impact strength decreased when the MWCNTs were added into the main hopper. However, with regard to the elongation at break, the high standard deviation has to be considered. The slight decrease in the notched impact strength was attributed to the higher number of small MWCNT

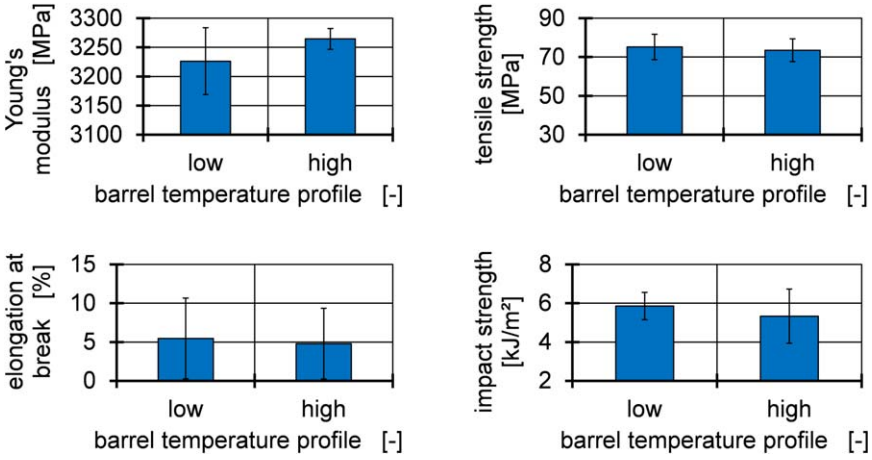

Figure 7. Mechanical properties of the nylon 6/MWCNT composites versus the barrel temperature profile. [Color figure can be viewed in the online issue, which is available at wileyonlinelibrary.com.]

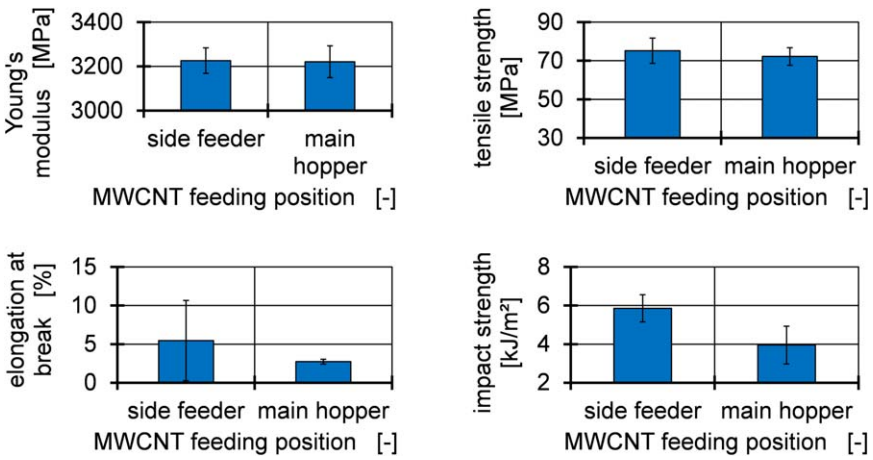

Figure 8. Mechanical properties of the nylon 6/MWCNT composites versus the MWCNT feeding position. [Color figure can be viewed in the online issue, which is available at wileyonlinelibrary.com.]

agglomerates, which occurred when the MWCNTs were fed into the main hopper. These agglomerates on a microscopic scale may have acted as defects during impact loading.

Only small influences of the melt-compounding process conditions on the mechanical properties were observed. The increase in the Young's modulus and the decrease in the notched impact strength, which occurred when certain process parameters were varied, could be attributed to the size and number of detected MWCNT agglomerates. However, the differences in the MWCNT agglomerate size distribution were not necessarily reflected in a variation of the mechanical properties. Thus, we concluded that the differences in the morphology were too small to affect the mechanical properties of the nylon 6/MWCNT composites substantially.

Rheology. Figure 9 shows the rheological properties, the complex viscosity, G', and G'', of the nylon 6/MWCNT composites versus the mass throughput [Figure 9(a)], the screw rotational speed [Figure 9(b)], the screw configuration [Figure 9(c)], the barrel temperature profile [Figure 9(d)], and the feeding position of the MWCNT [Figure 9(e)]. During the trials, the processing parameters that are not depicted in the figures were kept constant.

As expected, the complex viscosity of all of the nylon 6/MWCNT composites decreased, whereas G' and G'' increased with increasing frequency. However, up to a frequency of 10 Hz, a lower complex viscosity, G', and G'' were observed for the low throughput of 10 kg/h. This effect could have been to a degradation of the nylon 6 because of the longer residence time in the twin-screw extruder at the low mass throughput. Shorter polymer chains caused higher chain mobility and less intermolecular friction and, thus, led to a lower G' and G''.

The screw rotational speed did not substantially affect the rheological properties. Also, Sathyanarayana et al.[50] observed only a very small influence of the screw rotational speed on the rheological properties of the polystyrene/MWCNT composites up to a MWCNT content of 2 wt % in their study. However, at higher MWCNT contents, the complex viscosity and G' increased, when higher screw rotational speeds were applied.

Only very small differences in the rheological properties were observed when different screw configurations were used. This led to the conclusion that the applied screw configurations did not substantially influence the rheological properties.

A higher barrel temperature profile resulted in a slightly higher complex viscosity and in increased G' and G'' values. This may have been due to the improved dispersion of the MWCNTs at higher barrel temperatures. The improved MWCNT dispersion led to reduced polymer chain mobility and caused a higher elastic resilience and an increased intermolecular friction; this was reflected in the G' and G'' values. A similar observation was made by Pötschke et al.[47] for polycaprolactone/MWCNT composites, when the rotational speed was increased during mixing with laboratory-scale mixing equipment.

The addition of the MWCNTs into the main hopper resulted in a lower complex viscosity and decreases in G' and G''. This observation was attributed to the fact that the addition into the main hopper led to a compression of the MWCNTs in the feeding and melting zones of the extruder and resulted in new additional MWCNT agglomerates, as suggested by Müller et al.[56] The newly formed agglomerates caused a worse MWCNT dispersion and a higher polymer chain mobility and resulted in a lower complex viscosity. The deformation energy stored in the material and the inner friction were reduced as well, and this led to lower G' and G'' values. Additionally, mechanical deterioration of the MWCNTs may have occurred because of the three-flighted kneading blocks in the melting zone. According to Pötschke et al.,[47] the deterioration of the MWCNTs may have also resulted in a reductions of the complex viscosity and G'.

The investigated melt-compounding process parameters, the mass throughput, screw rotational speed, screw configuration, and barrel temperature, had only a very small and not very substantial effect on the rheological properties. Also, the differences observed in the morphology were not fully reflected in rheological properties; this led us to the conclusion that the differences

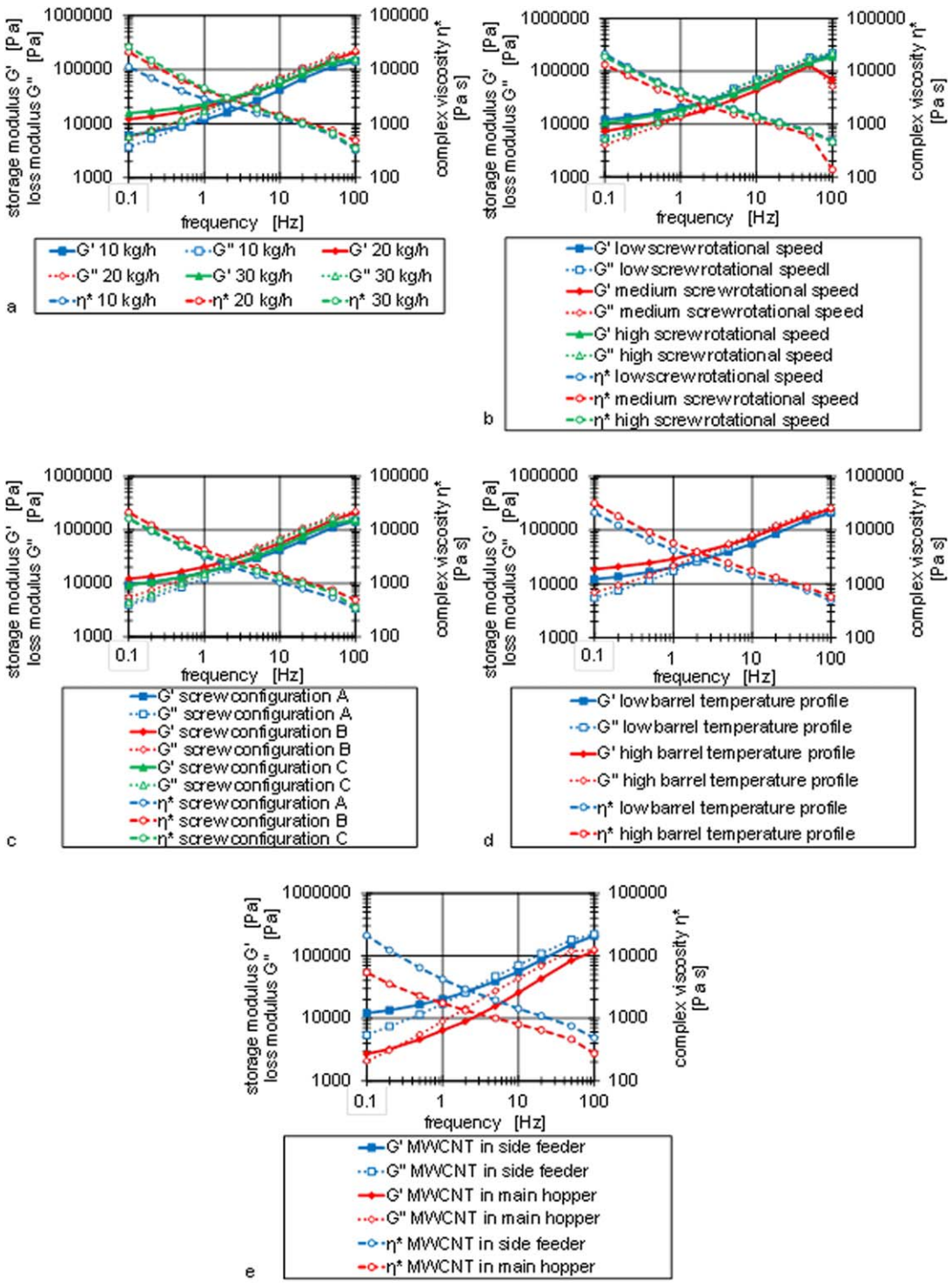

Figure 9. Rheological properties of the nylon 6/MWCNT composites versus the melt-compounding conditions. [Color figure can be viewed in the online issue, which is available at wileyonlinelibrary.com.]

in the morphology were too small to have an effect on the rheological properties. McClory et al.[57] and Miltner et al.[58] reported similar influences of the process parameter on the rheological properties of the polymer/MWCNT composites during small-scale mixing. Only the addition of MWCNTs into the main hopper instead through a side feeder substantially affected the rheological properties. This effect may have been due to a compression of the MWCNTs in the feeding and melting zone and caused additional agglomerates[56] and/or a mechanical deterioration of the MWCNTs.[47]

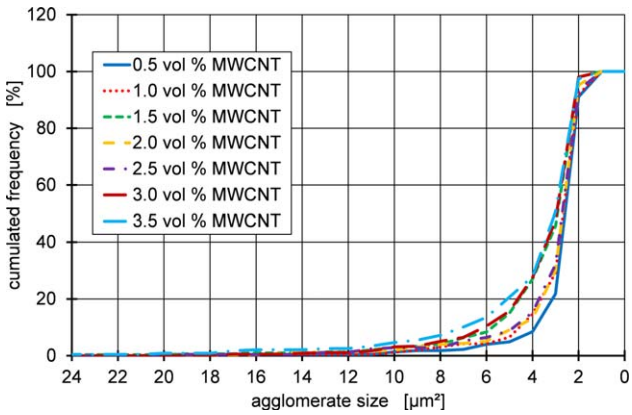

Figure 10. Cumulated MWCNT agglomerate frequency versus the MWCNT volume content. [Color figure can be viewed in the online issue, which is available at wileyonlinelibrary.com.]

Effect of the Nanotube Content

Morphology. Figure 10 depicts the accumulated MWCNT agglomerate frequency in the nylon 6/MWCNT composites. With increasing MWCNT content, larger agglomerates were observed slightly more often. However, 90% of the MWCNT agglomerates were smaller than 7 μm^2. At a MWCNT content of 0.5 vol %, 90% of the agglomerates were even smaller than 4 μm^2.

TEM images of the Nylon 6/MWCNT composites are shown in Figure 11.

In the TEM images prepared from tensile bars, the individual MWCNTs could be observed as wormlike structures, which were curved and wavy. The individual MWCNTs were randomly dispersed and showed no orientation or alignment in the tensile bar. Furthermore, MWCNTs longer than 500 nm were observed. Independently of the MWCNT volume content, no MWCNT aggregates were visible in the TEM images. Thus, the MWCNTs showed a relatively good and homogeneous dispersion in the nylon 6 matrix.

Mechanical Properties. In Figure 12, the mechanical properties of the nylon 6/MWCNT composites are depicted versus the MWCNT volume content.

Figure 12(a) shows that the Young's modulus increased with increasing MWCNT content. Furthermore, the Young's modulus of the nylon 6/MWCNT composites (Y) was modeled by the shear-lag model according to Cox[59] and modified by Krenchel[60] [eq. (3)]:

$$Y = (\eta_o \cdot \eta_l \cdot Y_{MWCNT} - Y_{Nylon6}) \cdot \nu_{MWCNT} + Y_{Nylon6} \quad (3)$$

with

$$\eta_l = 1 - \frac{\tanh(a \cdot l/d)}{a \cdot l/d} \quad (4)$$

and

$$a = \sqrt{\frac{-3 \cdot Y_{Nylon6}}{2 \cdot Y_{MWCNT} \cdot \ln(\nu_{MWCNT})}} \quad (5)$$

where Y_{MWCNT} and Y_{Nylon6} are the Young's moduli of the MWCNT and pure nylon 6, respectively; υ_{MWCNT} is the MWCNT volume content; η_o is the orientation factor, which was equal to 0.2 according to Krenchel;[60] l is the length of the MWCNTs, which was assumed to be 418 nm;[61,62] tanh stands for the hyperbolic tangent and d is the diameter of the MWCNTs, which was 9.5 nm according to the manufacturer.[53] The Young's modulus of the MWCNT was estimated with eq. (6):[63]

$$Y_{MWCNT} = \frac{4 \cdot t}{d} Y_{SWCNT} \quad (6)$$

where Y_{SWCNT} is the Young's modulus of the single-walled carbon nanotubes, which was given in the literature (1 TPa), and t

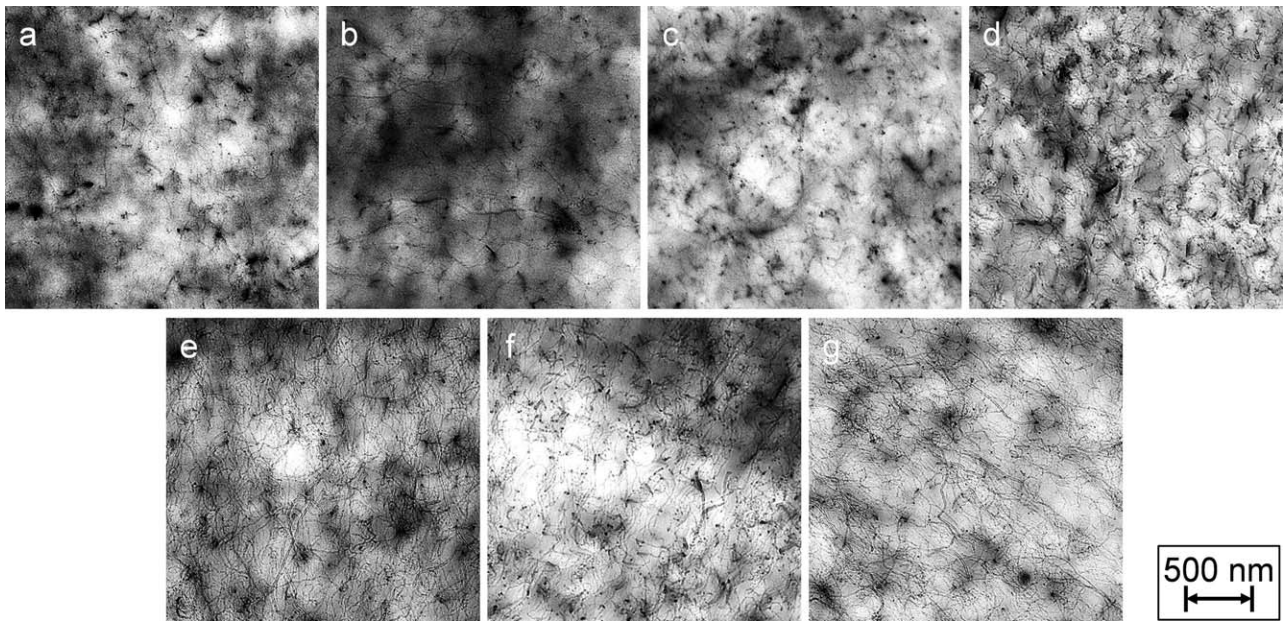

Figure 11. TEM images of the nylon 6/MWCNT composites versus the MWCNT volume content from (a) 0.5 to (g) 3.5 vol % MWCNTs increased in steps of 0.5 vol %.

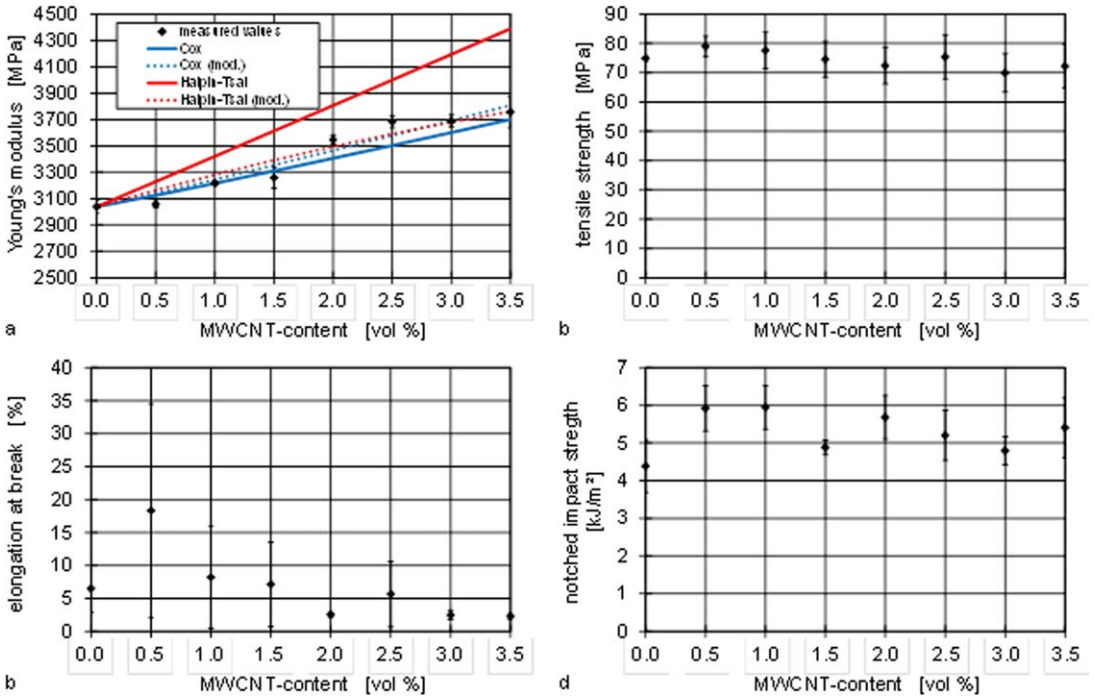

Figure 12. Mechanical properties of the nylon 6/MWCNT composites versus the MWCNT volume content. [Color figure can be viewed in the online issue, which is available at wileyonlinelibrary.com.]

is the thickness of the nanotubes, which was assumed to be the thickness of a single-atom-thick graphene layer (0.34 nm).[63] Equation (6) is valid for $t/d > 0.25$.[63] Thus, the Young's modulus of the MWCNTs was calculated to be 0.143 TPa. Additionally, the Young's modulus was modeled by the Halpin–Tsai model for randomly oriented fibers [eq. (7)]:[64]

$$Y = Y_{\text{Nylon6}} \cdot \left(\frac{3}{8} \cdot \left(\frac{(1+\xi \cdot \eta_L \cdot \nu_{\text{MWCNT}})}{(1-\eta_L \cdot \nu_{\text{MWCNT}})} \right) + \frac{5}{8} \cdot \left(\frac{(1+2 \cdot \eta_T \cdot \nu_{\text{MWCNT}})}{(1-\eta_T \cdot \nu_{\text{MMWCNT}})} \right) \right) \tag{7}$$

with

$$\eta_L = \frac{Y_{\text{MWCNT}}/Y_{\text{Nylon6}} - 1}{Y_{\text{MMWCNT}}/Y_{\text{Nylon6}} + \xi} \tag{8}$$

and

$$\eta_T = \frac{Y_{\text{MWCNT}}/Y_{\text{Nylon6}} - 1}{Y_{\text{MWCNT}}/Y_{\text{Nylon6}} + 2} \tag{9}$$

as well as

$$\xi = \frac{2 \cdot l}{d} \tag{10}$$

Because both models are well known, the derivations and backgrounds are not fully reproduced here. The Cox model reproduced the measured values well. A modification of the Cox model obtained by curve fitting slightly increased η_o from 0.20 to 0.23; this underlined the fact that the MWCNTs were randomly oriented in nylon 6, as shown by the TEM images (Figure 11). The Halpin–Tsai model led to much higher values for Young's modulus than the measurements of the tensile tests. Because the difference between the Young's modulus obtained by eq. (7) and the measured values increased linearly, a MWCNT efficiency factor was introduced [eq. (11)]:[65]

$$F(\nu_{\text{MWCNT}}) = 1 + \alpha \cdot \nu_{\text{MWCNT}} \tag{11}$$

The Halpin–Tsai equation [eq. (7)] was multiplied by the MWCNT efficiency factor. The decay factor (α) was obtained by curve fitting and calculated to be −4.08 for the nylon 6/MWCNT composites. From the negative decay factor, we concluded that the reinforcing efficiency of the MWCNT decreased with increasing MWCNT volume content.[65] Above a critical MWCNT volume content of 16.95 vol %, the Young's modulus of the nylon 6/MWCNT composites was lower than the Young's modulus of the neat nylon 6. This effect was attributed to a decreasing mean free path with increasing MWCNT volume content; this resulted in an increase of the attractive forces between the MWCNTs.[66] Furthermore, the MWCNT/MWCNT interactions were more likely to occur with increasing MWCNT volume content and to promote MWCNT degradation. In general, the obtained results were in good agreement with the studies of Meincke et al.[33] and Mahmood et al.[67]

The tensile strength only increased slightly at MWCNT contents of 0.5 and 1.0 vol %. A further increase in the MWCNT volume content led to a decrease in the tensile strength [Figure 12(b)]. This effect was probably due to the random orientation of the MWCNTs and their wormlike structure. Both substantially limited the potential of the MWCNTs as a reinforcing filler. Similar observations were made by Meng et al.[32] for nylon 6/MWCNT composites.

The elongation at break strongly increased with the addition of 0.5 vol % MWCNTs but decreased with the further addition of

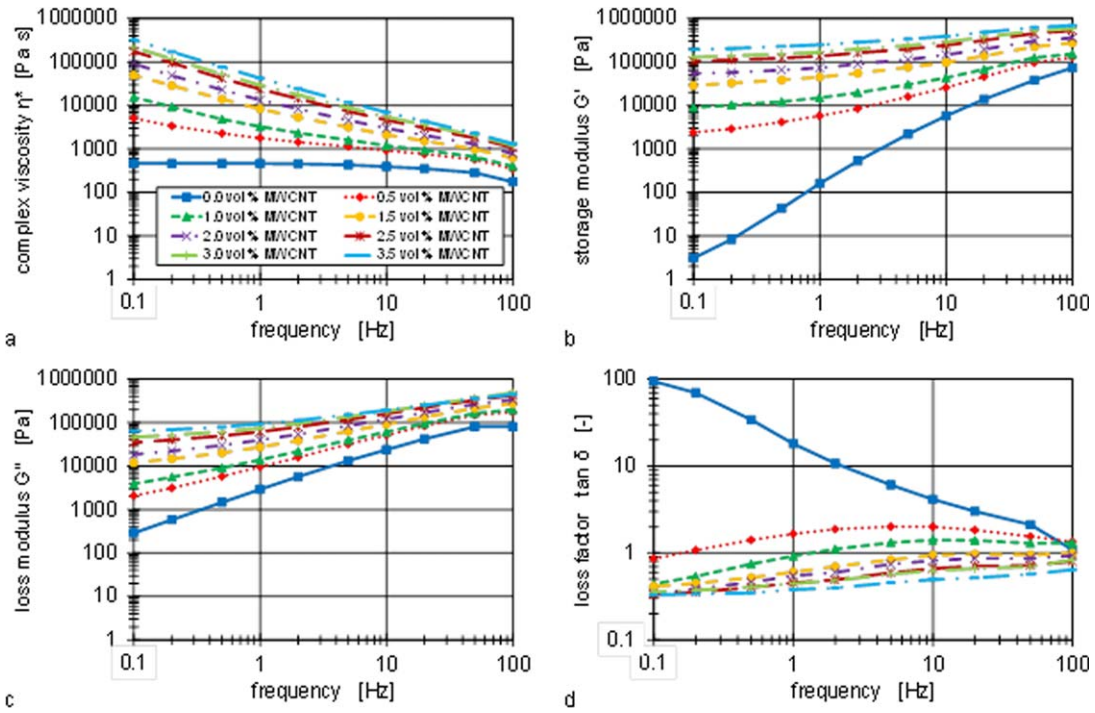

Figure 13. Rheological properties of the nylon 6/MWCNT composites versus the MWCNT volume content. [Color figure can be viewed in the online issue, which is available at wileyonlinelibrary.com.]

MWCNTs [Figure 12(c)]. An MWCNT content of 0.5 vol % did not restrict the chain mobility of the nylon 6 during plastic deformation, whereas a higher MWCNT volume contents embrittled the nylon 6; this was in good agreement with the literature.[30,31,67–70]

With the addition of 0.5 and 1.0 vol % MWCNTs, an increase of 1.6 kJ/m^2 in the notched impact strength ws observed [Figure 12(d)]. However, with the further addition of MWCNTs, the notched impact strength decreased, but it was still higher than the notched impact strength of the neat nylon 6. This led us to the conclusion that the MWCNT did not lead to an embrittlement of the nylon 6 during impact load. The MWCNTs resulted rather in a slight reinforcing effect perpendicular to the flow direction of the injection-molded test specimens; this was attributed to the randomly oriented MWCNTs.

Rheology. In Figure 13, the rheological properties of the nylon 6/MWCNT composites are depicted versus the frequency and the MWCNT volume content.

The complex viscosity of the nylon 6/MWCNT composites decreased with increasing frequency; this indicated a non-Newtonian pseudoplastic flow behavior of the nanocomposites [Figure 13(a)]. Wang et al.[35] made similar observations, which were attributed to an orientation and a restricted entanglement of the nylon 6 chains due to the presence of MWCNTs. Furthermore, an increase in the MWCNT volume content led to an increase in the complex viscosity, which was explained by more frequent MWCNT–MWCNT interactions and a restricted mobility of the polymer chains due to the MWCNTs. However, the increase in the complex viscosity decreased with increasing MWCNT volume content; this may have been due to an increased tendency of the MWCNTs to form agglomerates.

With regard to G' [Figure 13(b)] and G'' [Figure 13(c)], the neat nylon 6 exhibited the typical behavior of a homopolymer at low frequencies: The elastic portion (G') was rather small because of the fully relaxed polymer chains. With increasing shear deformation, both G' and G'' increased. However, an increase in the MWCNT volume content resulted in a reduction of the frequency dependency of G' and G'', even at low frequencies. This effect could be explained by strong MWCNT–MWCNT and MWCNT–nylon 6 interactions, which led to networklike structures, limited the mobility of the polymer chains, and resulted in the transition of a fluid to a more rubbery behavior because of the formation of a CNT network.[35,71–73]

This was also reflected in the loss factor (tan δ or G''/G') because a higher tan δ indicated a highly viscous behavior, whereas a low tan δ implied an ideal elastic behavior of the material [Figure 13(d)]. The observations made were in good agreement with the study of Wang et al.[35]

CONCLUSIONS

This study revealed that the melt-compounding conditions influenced the morphology on a microscopic scale, whereas for the mechanical properties, only small influences of the melt-compounding conditions were observed: increases in the mass throughput and the barrel temperature profile resulted in an increase in the Young's modulus and a decrease in the notched impact strength. These observations were attributed to the size and number of detected MWCNT agglomerates. Except for the MWCNT feeding position, no substantial effect of the melt-

compounding process parameters on the rheological properties of the nylon 6/MWCNT composites was observed. The feeding of the MWCNTs into the main hopper resulted in decreases in the complex viscosity, G', and G'', which may have been due to a compression of the MWCNTs in the feeding and melting zones, which resulted in additional agglomerates and/or a mechanical deterioration of the MWCNTs. However, the differences in the MWCNT agglomerate size distribution were not necessarily reflected in the variation of the mechanical or rheological properties. Thus, we concluded that the differences in the morphology were too small to affect most of the mechanical and rheological properties of the nylon 6/MWCNT composites.

Furthermore, the MWCNT volume content affected the dispersion of the MWCNTs slightly because a higher number of larger agglomerates was observed. This was due to a decrease in the mean free path between the agglomerates; this resulted in an increase of the attractive forces and a tendency to build agglomerates. The Young's modulus increased with increasing MWCNT volume content, whereas the tensile strength, elongation at break, and notched impact strength exhibited a maximum value around 0.5 to 1.0 vol %. This effect was attributed to the structure of the MWCNTs, their random orientation, and their increased tendency to form agglomerates with increasing MWCNT volume content. The investigations of the rheology showed that an increasing MWCNT volume content resulted in higher complex viscosities and G' and G'' values and a lower tan δ compared to those of neat nylon 6, especially at low frequencies. Moreover, the nylon 6/MWCNT composites exhibited a transition from a liquidlike to a solidlike viscoelastic behavior when the MWCNT volume content was increased.

ACKNOWLEDGMENTS

The authors thank Kevin Kistermann, Claudia Pütz, and Alexander Schwedt from the Gemeinschaftslabor für Elektronenmikroskopie of Rheinisch-Westfälische Technische Hochschule (RWTH) Aachen University for assistance with the SEM images. Furthermore, they thank Coperion GmbH, Stuttgart, Germany, and Arburg GmbH & Co. KG, Loßburg, Germany, for providing the machinery and BASF SE, Ludwigshafen, Germany, and Nanocyl S. A., Sambreville, Belgium, for supplying the material.

REFERENCES

1. Archawal, B. D.; Broutman, L. J.; Chandrashekhara, K. Analysis and Performance of Fiber Composites; Wiley: New York, **2006**.
2. Wu, S. H.; Wang, F. Y.; Ma, C. C.; Chang, W. C.; Kuo, C. T.; Kuan, H. C.; Chen, W. J. *Mater. Lett.* **2001**, *49*, 327.
3. Akkapeddi, M. K. *Polym. Compos.* **2000**, *21*, 576.
4. Iijima, S. *Nature* **1991**, *354*, 56.
5. Okada, A.; Kawasumi, M.; Kurauchi, T.; Kamigaito, O. *Polym. Prepr.* **1987**, *28*, 447.
6. Usuki, A.; Kojima, Y.; Okada, A.; Fukushima, Y.; Kurauchi, T.; Kamigaito, O. *J. Mater. Res.* **1993**, *8*, 1179.
7. Kojima, Y.; Usuki, A.; Kawasumi, M.; Okada, A.; Fukushima, Y.; Kurauchi, T.; Kamigaito, O. *J. Mater. Res.* **1993**, *8*, 1185.
8. Wypych, G. Handbook of Fillers; ChemTec: Toronto, Canada, **2010**.
9. Alig, I.; Pötschke, P.; Lellinger, D.; Skipa, T.; Pegel, S.; Kasaliwal, G. R.; Villmow, T. *Polymer* **2012**, *53*, 4.
10. Breuer, O.; Sundararaj, U. *Polym. Compos.* **2004**, *25*, 630.
11. Villmow, T.; Pötschke, P.; Pegel, S.; Häußler, L.; Kretzschmar, B. *Polymer* **2008**, *49*, 3500.
12. Thostenson, E. T.; Ren, Z.; Chou, T.-W. *Compos. Sci. Technol.* **2001**, *61*, 1899.
13. Lau, K. T.; Hui, D. *Compos. B* **2002**, *33*, 263.
14. Salvetat-Delmotte, J.-P.; Rubio, A. *Carbon* **2002**, *40*, 1729.
15. Andrews, R.; Weisenberger, M. C. *Curr. Opin. Solid State Mater.* **2004**, *8*, 31.
16. Harris, P. J. F. *Int. Mater. Rev.* **2004**, *49*, 31.
17. Xie, X.-L.; Mai, Y.-W.; Zhou, X.-P. *Mater. Sci. Eng. R-Rep.* **2005**, *49*, 89.
18. Coleman, J. N.; Khan, U.; Gun'ko, Y. K. *Adv. Mater.* **2006**, *18*, 689.
19. Coleman, J. N.; Khan, U.; Blau, W. J.; Gun'ko, Y. K. *Carbon* **2006**, *44*, 1624.
20. Lau, K.-T.; Gu, C.; Hui, D. *Compos. B* **2006**, *37*, 425.
21. Moniruzzaman, M.; Winey, K. I. *Macromolecules* **2006**, *39*, 5164.
22. Byrne, M. T.; Gun'ko, Y. K. *Adv. Mater.* **2010**, *22*, 1672.
23. Bose, S.; Khare, R. A.; Moldenaers, P. *Polymer* **2010**, *51*, 975.
24. Chou, T.-W.; Gao, L.; Thostenson, E. T.; Zhang, Z.; Byun, J.-H. *Compos. Sci. Technol.* **2010**, *70*, 1.
25. Ma, P.-C.; Siddiqui, N. A.; Marom, G.; Kim, J.-K. *Compos. A* **2010**, *41*, 1345.
26. Spitalsky, Z.; Tasis, D.; Papagelis, K.; Galiotis, C. *Prog. Polym. Sci.* **2010**, *35*, 357.
27. Jin, F.-L.; Park, S.-J. *Carbon Lett.* **2011**, *12*, 57.
28. Grady, B. P. *J. Polym. Sci. Part B: Polym. Phys.* **2012**, *50*, 591.
29. Jogi, B. F.; Sawant, M.; Kulkarni, M.; Brahmankar, P. K. *J. Encap. Adsorp. Sci.* **2012**, *2*, 69.
30. Zhang, W. D.; Shen, L.; Phang, I. Y.; Liu, T. *Macromolecules* **2004**, *37*, 256.
31. Liu, T.; Phang, I. Y.; Shen, L.; Chow, S. Y.; Zhang, W. D. *Macromolecules* **2004**, *37*, 7214.
32. Meng, H.; Sui, G. X.; Fang, P. F.; Yang, R. *Polymer* **2008**, *49*, 610.
33. Meincke, O.; Kämpfer, D.; Weickmann, H.; Friedrich, C.; Vathauer, M.; Warth, H. *Polymer* **2004**, *45*, 739.
34. Zhang, L.; Wang, C.; Zhang, Y. *Polym. Eng. Sci.* **2009**, *49*, 1909.
35. Wang, M.; Wang, W.; Liu, T.; Zhang, W.-D. *Compos. Sci. Technol.* **2008**, *68*, 2498.

36. Pötschke, P.; Fornes, T. D.; Paul, D. R. *Polymer* **2002**,*43*, 3247.
37. Andrews, R.; Jacques, D.; Minot, M.; Rantell, T. *Macromol. Mater. Eng.* **2002**, *287*, 395.
38. Pötschke, P.; Dudkin, S. M.; Alig, I. *Polymer* **2003**, *44*, 5023.
39. Pötschke, P.; Bhattacharyya, A. R.; Janke, A. *Eur. Polym. J.* **2004**, *40*, 137.
40. Schartel, B.; Pötschke, P.; Knoll, U.; Abdel-Goad, M. *Eur. Polym. J.* **2005**, *41*, 1061.
41. Pötschke, P.; Bhattacharyya, A. R.; Janke, A.; Pegel, S.; Leonhardt, A.; Täschner, C. *Fuller. Nanotubes Carbon Nanostruct.* **2005**, *13*, 211.
42. Dondero, W. E.; Gorga, R. E. *J. Polym. Sci. Part B: Polym. Phys.* **2006**, *44*, 864.
43. Lin, B.; Sundararaj, U.; Pötschke, P. *Macromol. Mater. Eng.* **2006**, *291*, 227.
44. Pötschke, P.; Häußler, L.; Pegel, S.; Steinberger, R.; Scholz, G. *Kautsch. Gummi Kunstst.* **2007**, *60*, 432.
45. Villmow, T.; Pegel, S.; Pötschke, P.; Wagenknecht, U. *Compos. Sci. Technol.* **2008**, *68*, 777.
46. Krause, B.; Pötschke, P.; Häußler, L. *Compos. Sci. Technol.* **2009**, *69*, 1505.
47. Pötschke, P.; Villmow, T.; Krause, B. *Polymer* **2013**, *54*, 3071.
48. Kasaliwal, G. R.; Pegel, S.; Göldel, A.; Pötschke, P.; Heinrich, G. *Polymer* **2010**, *51*, 2708.
49. Villmow, T.; Kretzschmar, B.; Pötschke, P. *Compos. Sci. Technol.* **2010**, *70*, 2045.
50. Sathyanarayana, S.; Olowojoba, G.; Weiss, P.; Caglar, B.; Pataki, B.; Mikonsaari, I.; Hübner, C.; Henning, F. *Macromol. Mater. Eng.* **2013**, *298*, 89.
51. Guehenec, M.; Tishkova, V.; Dagreou, S.; Leonardi, F.; Derail, C.; Puech, P.; Pons, F.; Gauthier, B.; Cadaux, P.-H.; Bacsa, W. *J. Appl. Polym. Sci.* **2013**, *129*, 2527.
52. N. N. Datasheet Ultramid B27E01 Polyamide 6, BASF SE, Ludwigshafen, Germany, **2010**.
53. N. N. Datasheet Nanocyl NC7000, Nanocyl S. A., Sambreville, Belgium, **2009**.
54. Schaffer, M. S. P.; Windle, A. H. *Adv. Mater.* **1999**, *11*, 937.
55. Kohlgrüber, K.; Wiedmann, W. Co-Rotating Twin-Screw Extruders; Hanser: Munich, **2008**.
56. Müller, M. T.; Krause, B.; Kretzschmar, B.; Pötschke, P. *Compos. Sci. Technol.* **2011**, *71*, 1535.
57. McClory, C.; Pötschke, P.; McNally, T. *Macromol. Mater. Eng.* **2011**, *296*, 59.
58. Miltner, H. E.; Watzeels, N.; Goffin, A.-L.; Duquesne, E.; Benali, S.; Dubois, P.; Rahier, H.; Van Mele, B. *J. Mater. Chem.* **2010**, *20*, 9531.
59. Cox, H. L. *Br. J. Appl. Phys.* **1952**, *3*, 72.
60. Krenchel, H. Fiber Reinforcement; Akademisk Forlag: Copenhagen, **1964**.
61. Krause, B.; Boldt, R.; Pötschke, P. *Carbon* **2011**, *49*, 1243.
62. Krause, B.; Villmow, T.; Boldt, R.; Mende, M.; Petzold, G.; Pötschke, P. *Compos. Sci. Technol.* **2011**, *71*, 1145.
63. Thostenson, E. T.; Chou, T.-W. *J. Phys. D: Appl. Phys.* **2003**, *36*, 573.
64. Halpin, J. C.; Kardos, J. L. *Polym. Eng. Sci.* **1976**, *16*, 344.
65. Jiang, Z.; Hornsby, P.; McCool, R.; Murphy, A. *J. Appl. Polym. Sci.* **2012**, *123*, 2676.
66. Arao, Y.; Yumitori, S.; Suzuki, H.; Tanaka, T.; Tanaka, K.; Katayama, T. *Compos. A* **2013**, *55*, 19.
67. Mahmood, N.; Islam, M.; Hameed, A.; Saeed, S.; Khan, A. K. *J. Compos. Mater.*, **2013**, *47*, 1.
68. Chen, G.-X.; Kim, H.-S.; Park, B. H.; Yoon, J.-S. *Polymer* **2006**, *47*, 4760.
69. Gao, J.; Zhao, B.; Itkis, M. E.; Bekyarova, E.; Hu, H.; Kranak, V.; Yu, A.; Haddon, R. C. *J. Am. Chem. Soc.* **2006**, *128*, 7492.
70. Zhao, C.; Hu, G.; Justice, R.; Schaefer, D. W.; Zhang, S.; Yang, M.; Han, C. C. *Polymer* **2005**, *46*, 5125.
71. Du, F.; Fischer, J. E.; Winey, K. I. *J. Polym. Sci. Part B: Polym. Phys.* **2003**, *41*, 3333.
72. Mitchel, C. A.; Bahr, J. L.; Arepalli, S.; Tour, J. M.; Krishnammorti, R. *Macromolecules* **2002**, *35*, 8825.
73. Sung, Y. T.; Han, M. S.; Song, K. H.; Jung, J. W.; Lee, H. S.; Kum, C. K.; Joo, J.; Kim, W. N. *Polymer* **2006**, *47*, 4434.